



Control of crystalline phases in magnetic Fe nanoparticles inserted inside a matrix of porous carbon

M.P. Fernández^{a,*}, D.S. Schmool^{b,c}, A.S. Silva^c, M. Sevilla^d, A.B. Fuertes^d, P. Gorria^a, J.A. Blanco^a

^a Dpto. de Física, Universidad de Oviedo, Calvo Sotelo, s/n, 33007 Oviedo, Spain

^b IN-IFIMUP, Universidade do Porto, Rua do Campo Alegre 687, 4169-007 Porto, Portugal

^c Dpto. de Física, Universidade do Porto, Rua do Campo Alegre 687, 4440-661 Porto, Portugal

^d Instituto Nacional del Carbon (CSIC), Apartado 73, 33080 Oviedo, Spain

ARTICLE INFO

Available online 3 May 2009

Keywords:

Nanoparticle

Exchange-bias

Superparamagnetism

Activated carbon

ABSTRACT

Two magnetic composites made up of Fe nanoparticles (Fe-NPs) embedded in a porous amorphous carbon matrix are presented. One of the samples, Fe-S-AC, was obtained with the aid of sucrose and the other, Fe-AC, in the absence of this substance. The XRD patterns show Bragg diffraction peaks associated with α -Fe and γ -Fe crystalline phases in the Fe-AC sample, while only peaks corresponding to the α -Fe phase are observed for Fe-S-AC powders. The Fe-NPs exhibit broad particle-size distributions for both samples, 5–50 nm for Fe-AC, whereas two populations (2–8 and 10–70 nm) for the Fe-S-AC composite are found. This fact gives rise to poorly defined blocking temperatures, as it can be deduced from the broad maxima observed in $M_{ZFC}(T)$ variations. In addition, $M(H)$ curves for both Fe-AC and Fe-S-AC samples reveal the existence of exchange-bias effect for $T < 60$ K, probably due to a magnetic coupling within a core/shell structure of the Fe-NPs, although this effect was observed to be less significant for Fe-S-AC.

© 2009 Elsevier B.V. All rights reserved.

1. Introduction

It is well established that when the size of magnetic particles is drastically reduced down to the nanometer length scale, independently of the shapes or forms of the samples, surface and interface effects become relevant, and superparamagnetic (SPM) effects come into view [1–3]. Moreover, the presence, morphology and composition of a non-magnetic matrix surrounding the nanoparticles (NPs) play an important role in those aspects related to the magnetic interactions between NPs [4]. Furthermore, these systems could display novel physical-chemical properties resulting in its suitability to be used in a large number of technological applications. However, the experimental techniques required for precisely determining the interfacial behaviour at the atomic scale have been recently developed. Hence, an intense research effort, focused in the accurate characterization of these NP-systems, is under way to completely understand the new emerging phenomena [5]. In this article, we report on the correlation between magnetic behaviour and morphology of two composites in which Fe nanoparticles (Fe-NPs) have been randomly dispersed in an amorphous porous carbonaceous matrix.

2. Experimental

The carbon matrix employed for the insertion of Fe-NPs is a commercial activated carbon (AC) (M30; Osaka Gas, Japan) [6]. Two types of Fe-carbon composites, denoted as Fe-AC and Fe-S-AC, were synthesized. For the preparation of the Fe-AC sample, the AC was impregnated with a solution of iron nitrate in ethanol, dried at 80 °C and then heat treated under N_2 up to 900 °C (heating rate: 3 °C/min) for 3 h. In the case of the Fe-S-AC composite, the synthesis took place in two steps: (i) the AC was impregnated with iron nitrate and heat treated at 900 °C, (ii) the sample obtained from the previous step was impregnated with a solution of sucrose in water, dried at 120 °C and heat treated under N_2 at 600 °C for 2 h. The percentages of Fe in both samples were determined by means of thermogravimetric analysis (TGA) in air up to 700 °C, being 16.8% for the Fe-AC sample and 8.8% for the Fe-S-AC sample. The introduction of sucrose was previously found to be useful to protect Ni NPs against acid environments [7,8]. The textural properties of the AC sample and the composites (Fe-AC and Fe-S-AC) determined by nitrogen physisorption (ASAP 2010) are listed in Table 1.

The crystal structure of Fe-NPs was analysed by means of room temperature X-ray powder diffraction (XRD) using Cu K_α radiation ($\lambda = 1.5418$ Å) in the 2θ range 40°–160°. Transmission electron microscopy (TEM) was used to study the morphology of the samples and to estimate the NP size distributions. Magnetization

* Corresponding author. Tel.: +34 985105014; fax: +34 985103324.

E-mail address: fernandezpaz.uo@uniovi.es (M.P. Fernández).

Table 1
Textural properties of activated carbon and the synthesized composites.

Sample	BET surface area (m ² g ⁻¹)	Pore volume (cm ³ g ⁻¹)	Maximum of the pore size distribution (nm)
AC	2350	1.5	2.5
Fe-AC	750	0.6	2.5
Fe-S-AC	360	0.4	2.5

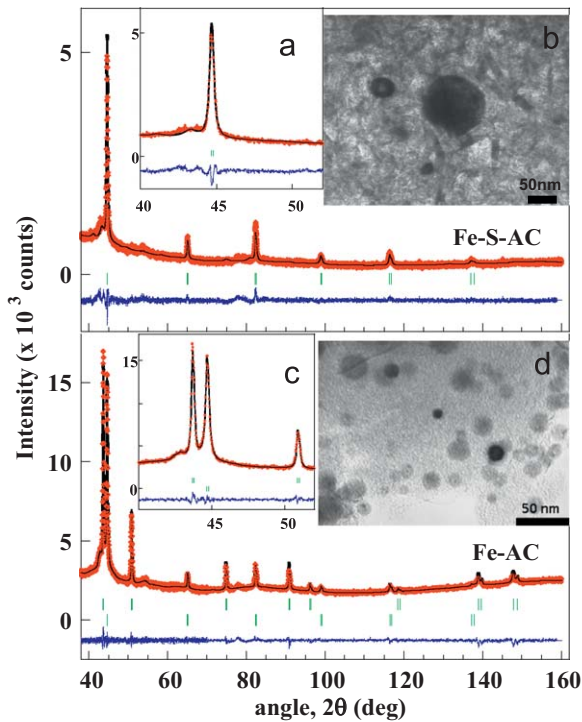


Fig. 1. Observed (points) and calculated (solid line) room temperature X-ray powder diffraction patterns of Fe-S-AC and Fe-AC composites. Positions of Bragg reflections are represented by vertical bars. The observed-calculated difference pattern is depicted at the bottom of each figure. In Fe-S-AC, the first series of vertical marks corresponds to α -Fe. In Fe-AC, the first series of vertical marks is associated with γ -Fe and the second with α -Fe. Insets (a) and (c) show the detail in 2θ -range around 45° to clearly appreciate the highest intensity Bragg reflections of the spectra. Insets (b) and (d) show TEM images of Fe-S-AC and Fe-AC, respectively. (For interpretation of the references to colour in this figure legend, the reader is referred to the web version of this article.)

vs. temperature, $M(T)$, curves in zero-field-cooling (ZFC) and field-cooling (FC) regimes, and under an applied magnetic field, $\mu_0 H = 1$ mT, were measured using a SQUID magnetometer in the temperature range from 5 to 370 K. Magnetization vs. magnetic fields, $M(H)$ cycles, were measured up to $\mu_0 H = \pm 2$ T at several selected temperatures. Low temperature $M(H)$ cycles were performed following two different procedures: cooling from 300 K down to 10 K under $\mu_0 H_{cool} = 2$ T ($M(H)$ @FC) and $\mu_0 H_{cool} = 0$ T ($M(H)$ @ZFC).

3. Results and discussion

Fig. 1 shows the room temperature XRD patterns corresponding to the Fe-S-AC (upper panel) and Fe-AC (bottom panel). The Rietveld refinement of the patterns has been performed using the Fullprof package [9]. Both XRD patterns exhibit broad diffraction peaks together with a large background contribution coming from the disordered and complex AC matrix [10] (note that both composites contain more than 80% of that

substance). The whole profile fit of the diffraction patterns (following the procedure explained in [11] for nanostructured systems) has been carried out by considering the same background contribution. The diffraction peaks displayed by the Fe-AC sample were indexed as the Bragg reflections of a body-centred cubic (bcc) and a face-centred cubic (fcc) crystal structures with lattice parameters $a = 2.867(1)$ and $3.587(1)$ Å, respectively (see inset c in Fig. 1). The former corresponds to an α -Fe phase while the latter can be identified as a γ -Fe phase, with relative percentages around 45(5)% (α) and 55(5)% (γ). However, the XRD pattern of Fe-S-AC composite suggests that only the α -Fe phase is present, with the same value for the lattice parameter, although we cannot completely discard the existence of traces (<5%) of γ -Fe phase (see Fig. 1a).

The average diameter value of the Fe-NPs in both composites has been estimated after the evaluation of several TEM images, from which a large number of NPs (>1500) have been counted. Representative TEM images are shown in the insets (b) and (d) of Fig. 1. The analysis of TEM images reveals that the Fe-AC sample contains a unique broad size distribution of Fe-NPs that follows rather well a log-normal function with an average NP size $\langle \tau \rangle = 15.4$ nm, and a standard deviation $\sigma = 6$ nm, as it has been previously reported [12]. On the other hand, the analysis of TEM images of Fe-S-AC sample clearly shows the existence of Fe-NPs with two different particle-size ranges: a sharp distribution (2–8 nm) with an average NP size $\langle \tau(\sigma) \rangle = 3(1)$ nm and another broad size distribution ranging from 10 to 70 nm and centred around $\langle \tau(\sigma) \rangle = 38(22)$ nm.

In Fig. 2 $M(H)$ @ZFC of Fe-AC and Fe-S-AC composites recorded at 10 K are displayed. To better compare the magnetic field dependence of the magnetization in both samples, the values of M have been normalized to those measured at $\mu_0 H = 2$ T, M/M_{2T} . From the saturation magnetization, M_s , at $T = 10$ K, we estimate a value of $M_s \approx 200$ Am² kg⁻¹, for α -Fe phase in both Fe-AC and Fe-S-AC samples, taking into account: (i) the different percentages of Fe

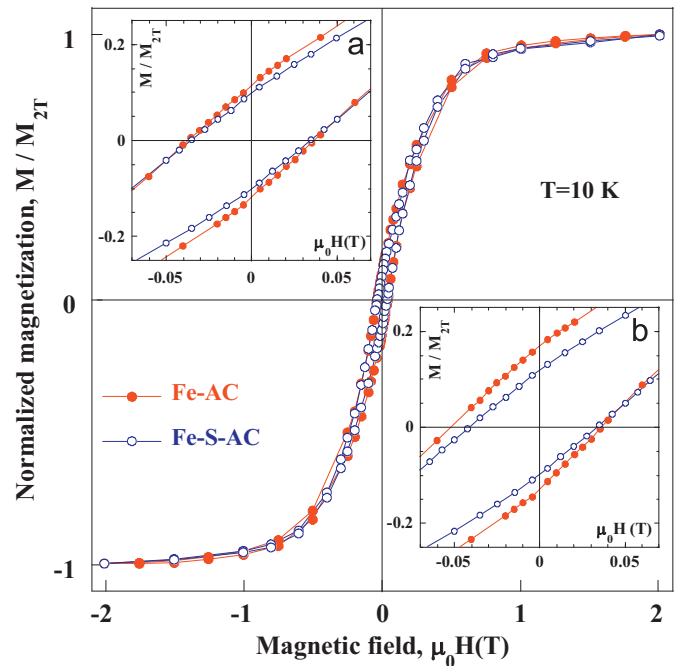


Fig. 2. $M(H)$ @ZFC measured at 10 K for Fe-AC (red full circles) and Fe-S-AC (blue open circles) samples. M_{2T} is the value of the magnetization for $\mu_0 H = 2$ T. Insets (a) and (b) display enlarged views of the $M(H)$ @ZFC and $M(H)$ @FC around $M/M_{2T} = 0$, respectively (see text). (For interpretation of the references to colour in this figure legend, the reader is referred to the web version of this article.)

Download English Version:

<https://daneshyari.com/en/article/1801427>

Download Persian Version:

<https://daneshyari.com/article/1801427>

[Daneshyari.com](https://daneshyari.com)